

Synthesis and Exciton Dynamics of Triplet Sensitized Conjugated Polymers

Rolf Andernach,^{†,#} Hendrik Utzat,^{†,‡,#} Stoichko D. Dimitrov,[†] Iain McCulloch,^{†,§} Martin Heeney,^{*,†} James R. Durrant,^{*,†} and Hugo Bronstein^{*,||}

[†]Centre for Plastic Electronics, Imperial College London, London, United Kingdom SW7 2AZ

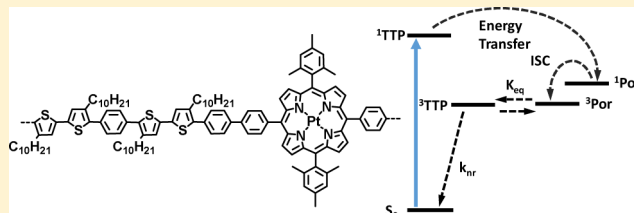
[‡]Department of Chemistry, Massachusetts Institute of Technology, Cambridge, Massachusetts 02139, United States

[§]SPERC, King Abdullah University of Science and Technology, Thuwal 23955-6900, Saudi Arabia

^{||}Department of Chemistry, University College London, London, United Kingdom WC1H 0AJ

Supporting Information

ABSTRACT: We report the synthesis of a novel polythiophene-based host–guest copolymer incorporating a Pt–porphyrin complex (TTP–Pt) into the backbone for efficient singlet to triplet polymer exciton sensitization. We elucidated the exciton dynamics in thin films of the material by means of Transient Absorption Spectroscopy (TAS) on multiple time scales and investigated the mechanism of triplet exciton formation. During sensitization, singlet exciton diffusion is followed by exciton transfer from the polymer backbone to the complex where it undergoes intersystem crossing to the triplet state of the complex. We directly monitored the triplet exciton back transfer from the Pt–porphyrin to the polymer and found that 60% of the complex triplet excitons were transferred with a time constant of 1087 ps. We propose an equilibrium between polymer and porphyrin triplet states as a result of the low triplet diffusion length in the polymer backbone and hence an increased local triplet population resulting in increased triplet–triplet annihilation. This novel system has significant implications for the design of novel materials for triplet sensitized solar cells and upconversion layers.



INTRODUCTION

Photoexcited states in organic semiconductors, termed excitons, can have two spin states: a singlet state and a triplet state. In the triplet state, the projections of the respective spin momenta on a given axis are aligned in parallel preventing them from occupying the same space, and hence, they experience reduced Pauli repulsion. This results in an overall lower energy of the triplet state compared to the singlet.¹ While the optical transitions between singlet states are typically allowed, the respective transitions between singlet and triplet states are spin-forbidden. Therefore, singlet excitons are normally the primary photoexcitations in organic semiconductors as triplet states cannot be accessed by excitation directly. Their ease of access has allowed singlet excitons to be studied extensively in organic semiconductors. Spectroscopic techniques are routinely employed to measure their properties such as energy levels, lifetime and diffusion length, and thus opened the door for organic semiconductors to be used in optoelectronic devices.

Triplet excitons are, however, of great importance in many optoelectronic devices. In OLEDs, a statistical ratio of 3:1 triplets to singlets is electrically generated via nongeminate hole and electron recombination, potentially limiting their efficiency due to the nonemissive nature of the polymer triplets. The incorporation of heavy metal complexes with high phosphorescence quantum yields can allow the utilization of up to 100% of excitons through the concept of energy harvesting whereby

all the excitons are transferred to the metal complex where they can subsequently decay radiatively (phosphorescence) due to the large spin orbit coupling of the heavy metal atom.^{2,3} One drawback, however, shows at high current densities where reductions in efficiency have been observed due to triplet–triplet annihilation.⁴

In polymer:fullerene bulk heterojunction solar cells, population of the polymer triplet state is considered a main loss mechanism. It has been shown that Charge-Transfer (CT) States, electron–hole pairs bound across the polymer:fullerene interface, can irreversibly recombine to form polymer triplet excitons due to their lower energy relative to the CT state.^{5–11} Furthermore, the presence of triplet excitons has been linked to the lifetime and stability of conjugated polymers both in neat film and in BHJ devices due to their quenching by oxygen potentially forming highly reactive oxygen species.¹² Triplet excitons can however be used for the generation of photocurrent when energy levels are appropriately aligned. It has been recently demonstrated for pentacene-based devices utilizing singlet fission that 100% quantum efficiencies can be surpassed. This is possible as singlet fission allows the conversion of one singlet into two triplet excitons each of which is capable of generating charges.^{13–16} In addition, the

Received: June 15, 2015

Published: July 22, 2015

incorporation of triplet–triplet annihilation (TTA) upconversion layers allow the conversion of IR radiation, normally wasted in solar cells due to their transparency in this wavelength region, into higher energy singlet excitons that are able to generate photocurrent.^{17–19} Despite the ubiquitous presence of triplet excited states in optoelectronic devices, neither the yield, energetic position nor mobility of polymer triplet excitons is routinely measured, partially due to the challenges of experimentally and theoretically accessing these states.^{20,21}

Understanding and controlling the properties of triplet excitons is a key consideration to allow polymers to be used in the next generation of optoelectronic devices. Of particular interest is the determination of polymer triplet exciton mobility. It has been suggested that the longer lifetime of triplet excitons could lead to a longer diffusion length than that of their singlet counterparts.^{22–26} Theoretical predictions have in fact suggested that an enhanced diffusion length could even be achieved with significant disorder present in the system.²⁷ Achieving an enhanced exciton diffusion length would allow for the construction of efficient bilayer organic photovoltaic devices, therefore negating the use of the complicated bulk heterojunction.^{22,23,25,26} Conversely, due to the slower Dexter type nature of the triplet energy transfer, triplet excitons have also been suggested to possess lower mobilities than their singlet counterparts. In triplet–triplet annihilation upconversion layers, a lower exciton mobility could be utilized to induce higher local exciton population thus increasing the collision encounter probability.

Experimentally, there have been few reports of triplet exciton diffusion lengths in organic semiconductors.²⁸ The hole transport material *N,N'*-di(1-naphthyl)-*N,N'*-diphenyl-(1,1'-biphenyl)-4,4'-diamine (NPD) has recently been reported to show a triplet diffusion length of 87 nm,²⁹ whereas the triplets in structurally related 4,4'-bis(carbazol-9-yl)1,1'-biphenyl (CBP) have been reported to have diffusion lengths of 12, 25, and 250 nm.^{30–32} C₆₀ was found to possess a triplet diffusion length of 30–35 nm,³³ and pentacene, which has been extensively studied for its ability to undergo singlet fission, has been shown to have a triplet diffusion length of 40 nm.³⁴ In contrast, structurally related rubrene has been reported to have a triplet diffusion length of 4 μm in a single crystal.³⁵ For polymeric systems, we are aware of only four literature values of triplet exciton mobility. Samiullah et al. reported a triplet diffusion length of almost 4 μm in a ladder-type polymer (PhLPPP).³⁶ Rand et al. reported both the triplet diffusion length of a poly phenylenevinylene polymer to be 9 nm (as compared to the 4 nm singlet diffusion length).^{22,23} Tamai et al. very recently determined the triplet diffusion lengths of two fluorene based polymers to be 0 and 41 nm.³⁷ It is worth noting how much the triplet properties of two such related structures can differ, highlighting the difficulty as well as the importance of creating the toolset necessary to systematically investigate triplet excited state properties. For polymer based optoelectronic devices to attain their ultimate efficiency and stability, the nature of the triplet exciton must be understood, especially in the next generation of OPV devices and TTA upconversion layers where control over triplet exciton mobility is the key to their success. Consequently, it would be of considerable interest to possess a class of materials where photoexcitation results in a high population of the triplet excitons, thus allowing for their detailed study and potential exploitation.

One approach to access the triplet state in the polymer from the photoexcited singlet state is to blend the polymer with heavy metal complexes, which allow the conversion of the singlet to the triplet state due to the strong spin orbit coupling of the heavy metal. For this to occur, careful consideration of the polymer and metal complex energy levels must be taken. The emission of the polymer must overlap with the absorption of the metal complex to allow for efficient energy transfer. Subsequently, the triplet energy level of the polymer must be below that of the complex to allow for back transfer of the triplet excitons (Figure 1). This approach has been

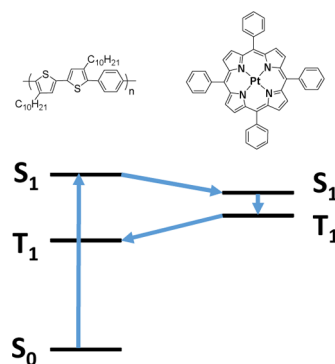


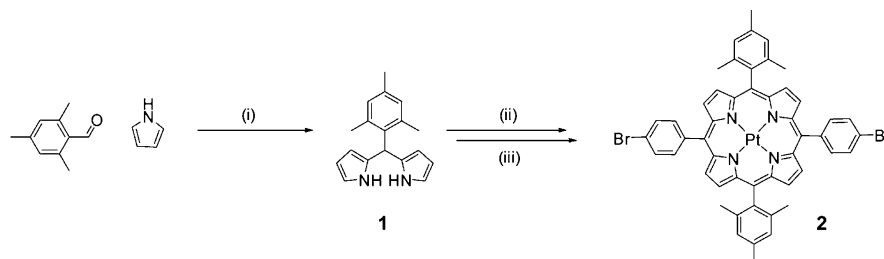
Figure 1. Triplet sensitization of a conjugated polymer using a heavy metal complex.

demonstrated previously, with the aim of producing triplet-sensitized solar cells.^{22,24,38,39} However, it has been demonstrated that blends of typically amorphous polymers and highly crystalline metal complexes often lead to extensive phase segregation resulting in a nonhomogenous distribution of the metal complex.^{40–43} Furthermore, this aggregation can result in undesirable exciton annihilation processes.^{43,44}

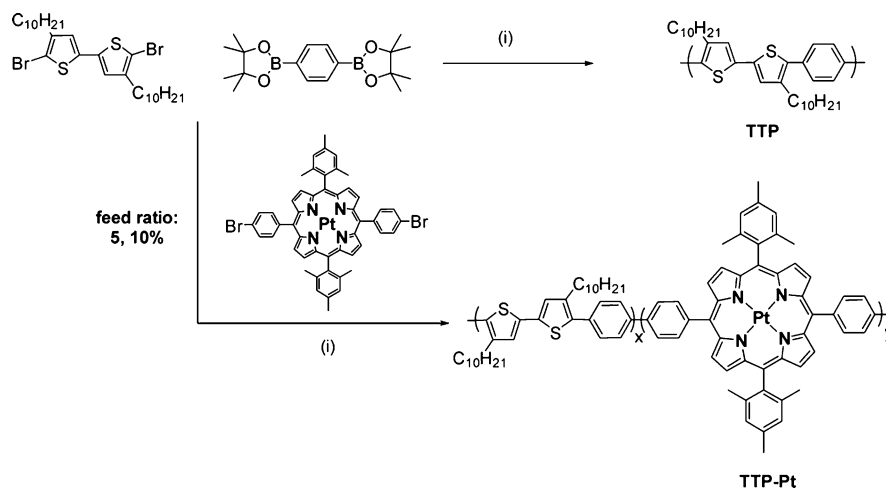
To overcome these issues, we report here the synthesis and photophysical characterization of a novel polythiophene polymer which includes a Pt–porphyrin complex in the backbone to create a triplet-sensitized conjugated polymer. Our material system allows for the tuning of the incorporation ratio of Pt–porphyrin in the polymer host and for the in-depth study of both singlet and triplet exciton formation. Incorporation of the metal complex into the polymer backbone prevents phase segregation while also simplifying film formation by removing the necessity of blending the two components and may also enhance the energy transfer mechanisms via direct orbital overlap. Furthermore, porphyrins typically show low solubility; incorporation into the polymer backbone circumvents any potential processing issues which can arise as a result of this.

RESULTS AND DISCUSSION

The synthesis of the polymers is shown in Schemes 1 and 2. Mesityldipyromethane (1) was obtained through a Lewis acid catalyzed condensation reaction of mesitaldehyde in an excess of pyrrole, leading to a white, sheet-like solid. The dipyromethane was reacted to form the platinated 10,20-dibromophenyl-5,15-dimesitylporphyrin (2) in two steps. Reaction of (1) with 4-bromobenzaldehyde proceeded at low concentrations (~5 mM), favoring the ring closure over linear side reactions; aromatization of the porphyrin cores was achieved using the oxidizing agent DDQ. The free base was then reacted with PtCl₂, forming the corresponding platinum porphyrin

Scheme 1. Synthesis of the Porphyrin Precursor^a

^aConditions: (i) MgBr₂, TFA, DCM, 50%; (ii) (a) DCM, TFA, (b) DDQ, 11%; (iii) PhCN, PtCl₂, reflux, 24%.

Scheme 2. Synthesis of the TTP and Pt–TTP Polymers^a

^aConditions: (i) Pd(PPh₃)₄, base, toluene, Ar, 115 °C.

complex. The mesityl substituents were chosen so as to impart solubility to the porphyrin and the final polymer, as well as to minimize porphyrin aggregation in the solid state, mediated by the out-of-plane twisting of the meso-substituents.

We chose the medium band gap conjugated backbone poly(phenyl-bithiophene) (TTP) for this study in order to ensure that all the energetic requirements for triplet-sensitization could occur efficiently. The TTP polymer was synthesized by Suzuki polymerization of 5,5'-dibromo-3,3'-didecyl-2,2'-bithiophene with 1,4-benzenediboronic acid bispinacolic ester (Scheme 2). The porphyrin-containing polymers (TTP–Pt) were synthesized via a Suzuki ter-molecular polymerization, with the different feed ratios and properties given in Table 1. Ter-molecular polymerizations have previously been used to optimize and explore the effects of specific monomers in conjugated polymers.⁴⁵

Table 1. Properties of Novel Polymers

	M_n [kDa] ^a	M_w [kDa] ^a	PDI	F_R [w %] ^b	I_R [mol %] ^c	I_R [w %] ^c
TTP	44.1	73.0	1.65	0%	0%	0%
TTP–Pt5	10.8	19.0	1.75	5%	2%	3%
TTP–Pt10	14.5	24.6	1.70	10%	5%	8%

^aDetermined by GPC using a polystyrene standard. ^bFeed ratio (F_R) determined by weight per repeat unit. ^cIncorporation ratios (I_R) determined by integration of the ¹H NMR porphyrin signal per repeat unit (referenced to the integral of the thiophene aromatic signal).

TTP was isolated as a bright yellow solid with high visible fluorescence, whereas all the porphyrin containing polymers were visibly less fluorescent. Reasonable molecular weights were obtained for all the resulting polymers, with a trend for decreasing molecular weight at higher porphyrin dopant ratios. We believe this to be due to a slight loss in solubility for the resulting polymers which resulted in a quicker precipitation of the polymer chains during the synthesis. We note the lower molecular weight of the porphyrin containing polymers may affect their photophysical properties somewhat, but we believe that due to the low molecular weight of the repeat units the degree of polymerization is sufficiently high for them to be considered polymeric. The incorporation of the platinum porphyrin was verified by ¹H NMR spectroscopy (Supporting Information S2), the aromatic signals of the thiophene (7.70 ppm) and phenyl groups (7.51 ppm) clearly attributed and their integrals matching. The porphyrin peaks (8.9–8.0 ppm) of the 10 w % doped polymer can be seen in comparison, with each peak integral corresponding to four protons on the porphyrin substructure. In the polymers containing higher weight percentages of porphyrin, a secondary smaller set of porphyrin peaks can be observed. This is likely to be due to a terminal porphyrin on the polymer chain as opposed to the above species which are incorporated into the conjugated polymer on both sides. Overall, the incorporation ratio of the porphyrin was slightly lower than the feed ratio for all concentrations which possibly stems from a lower reactivity of the porphyrin monomer relative to the bithiophene species.

Figure 2 displays the UV–vis spectra of TTP, TTP–Pt-5, and TTP–Pt-10 polymers in solution and thin films spin-

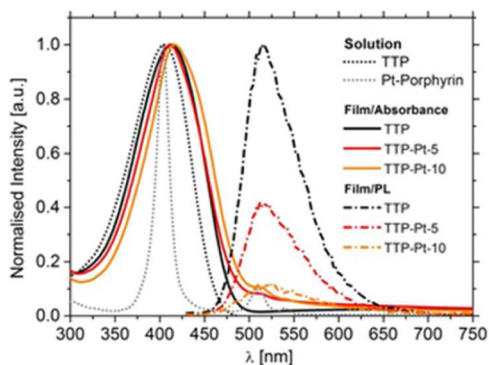


Figure 2. Absorption and emission spectra of novel polymers.

coated on glass. All thin film spectra are weakly red-shifted compared to the solution, likely because of solid state packing effects commonly observed in conjugate polymers (404 nm compared to 419 nm for TTP). The absorption maximum of the TTP polymer and the TTP–Pt5 and TTP–Pt10 polymers is around $\lambda_{\text{max}} = 416$ nm and have similar onset of polymer absorption. These findings indicate that the addition of the Pt–porphyrin complex and the difference in molecular weight, as determined by GPC, has no noticeable effect on the effective conjugation length of the polymer. The Pt–porphyrin complex exhibits two distinct absorption features around 405 and at 510 nm. The polymers show emission around 525 nm which we assign to the fluorescence of the TTP backbone. Both the absorption and emission energies are consistent with previously reported values for TTP.^{46,47} With increasing content of Pt–porphyrin in the backbone, the fluorescence intensity decreases (Figure 2), indicating an efficient singlet exciton quenching, which we tentatively assign to quenching induced by the Pt–porphyrin in the conjugated backbone.

In order to study the singlet and triplet exciton dynamics and the mechanism of the triplet exciton formation in TTP, TTP–Pt-5 and TTP–Pt-10, we used Transient Absorption Spectroscopy (TAS) on multiple time scales. First, we performed microsecond TAS of the polymer thin films spin-coated on glass to determine the triplet exciton yields and triplet exciton decay dynamics in the three polymers studied. Figure 3A presents the TAS spectra in the visible spectral region at 800 ns after photoexcitation of the TTP backbone (420 nm) for TTP, TTP–Pt-5, and TTP–Pt-10. The corresponding decays of the transient absorption are presented in Figure 3B. For TTP, TTP–Pt-5, and TTP–Pt-10, a similarly broad transient absorption signal at around 800 nm is observed. This signal is strongly quenched by the presence of oxygen for all samples, as it is shown for TTP–Pt-10 in the inset of Figure 3B. The decay of the transient absorption of the pristine TTP polymer was fitted well with a monoexponential function with $\tau_{\text{TTP}} = 501 \pm 3$ ns. Therefore, based on the similarity of the spectra and the observed oxygen quenching, we assign the signal to the transient absorption of the triplet exciton on the TTP backbone. Previously, Ohkita et al. reported the transient absorption maximum of the TTP polymer triplet exciton around 700 nm which is in close agreement with our observed value.⁴⁶

A comparison of the transient absorption between the three polymers reveals a clear increase of the initial signal amplitude

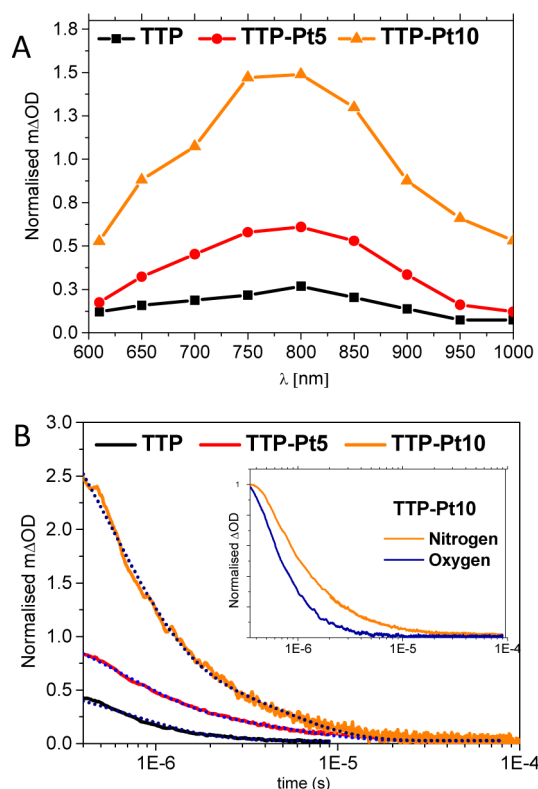


Figure 3. Transient absorption spectra of TTP, TTP–Pt-5, and TTP–Pt-10 measured at 800 ns after photoexcitation (420 nm) (A) and the corresponding decay dynamics measured at 800 nm (B). The inset in (B) shows the effect of moving from a nitrogen atmosphere (used for all experiments unless otherwise stated) to oxygen for TTP–Pt-10. Analogous acceleration of decay dynamics in the presence of oxygen were observed for all three polymers.

with increasing incorporation of Pt–porphyrin, demonstrating improved triplet generation yield. In addition, a change in the decay dynamics of the triplet exciton of TTP–Pt-5 and TTP–Pt-10 compared to the nonporphyrin containing TTP polymer is observed. While the decay of the triplet exciton of TTP follows a monoexponential dynamics, the relaxation of the triplet exciton in the TTP–Pt polymers can only be fitted with biexponential functions yielding $\tau_{1\text{-TTP-Pt5}} = 440 \pm 3$ ns and $\tau_{2\text{-TTP-Pt5}} = 3.55 \pm 0.03$ μ s; $\tau_{1\text{-TTP-Pt10}} = 380 \pm 3$ ns and $\tau_{2\text{-TTP-Pt10}} = 3.16 \pm 0.03$ μ s. The μ s decay component is not associated with any spectral evolution. In the course of our discussion, we will provide a possible explanation for the altered exciton decay dynamics of the TTP–Pt polymers compared to the TTP polymer.

In order to elucidate the singlet exciton dynamics and the triplet exciton formation, we utilized ultrafast TAS to measure thin films of TTP, TTP–Pt-5, and TTP–Pt-10. The spectra of TTP and TTP–Pt-10 up to 5.8 ns are presented in Figure 4.

The spectra of the neat TTP polymers exhibit three characteristic features. First, a negative, quickly relaxing transient absorption at around 525 nm is observed, disappearing on the 10–100 ps time scale. Comparison to the steady state PL spectra (see Figure 2) allows us to assign this feature to stimulated emission from the TTP singlet exciton. Second, a strong, fast decaying transient absorption in the red spectral region is observed. This transient absorption signal can be assigned to absorption of the singlet exciton of the TTP backbone which exhibits an absorption maximum in the

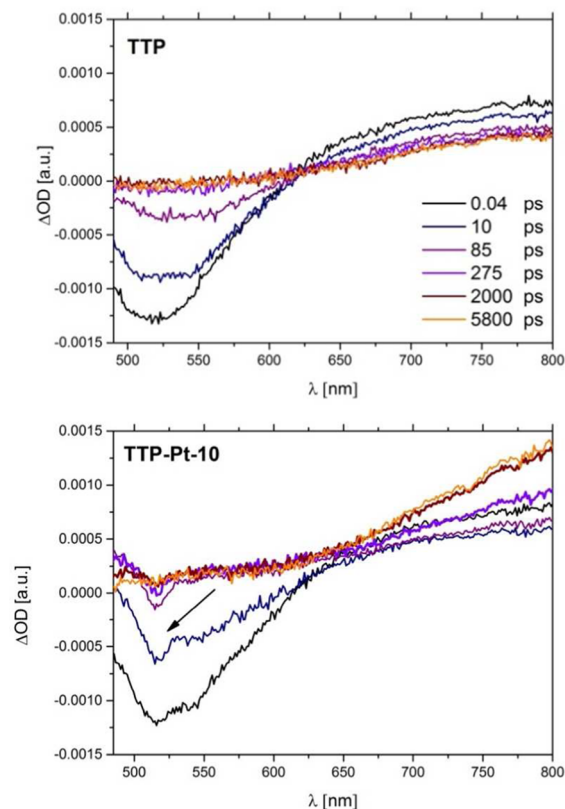


Figure 4. TAS spectra of TTP and TTP–Pt-10 films at delay times of 0.04–5800 ps after photoexcitation of the TTP (λ_{exc} : 420 nm).

near IR spectral region (see Supporting Information S3). Following the rapid decay of these two signals, assigned to singlet exciton decay, a residual broad transient absorption with increasing amplitude from 500 to 800 nm is observed, which does not evolve over the time scale measured (up to 5.8 ns after photoexcitation). This broad, long-lived transient absorption matches the spectral shape of the triplet exciton absorption measured at 800 ns delay (Figure 3 A) after photoexcitation and can thus be assigned to the triplet exciton on the TTP backbone.

The spectra of the TTP–Pt-10 polymer exhibit similar features as the TTP polymer, but an additional negative, relatively narrow transient absorption feature is observed at around 510 nm, most prominently in the spectra at time delays of 85 and 275 ps, as shown in Figure 4 (arrow). We assign this feature to the ground state bleach (GSB) of the Pt–porphyrin (compare to GS spectrum in Figure 2). We note that ISC from singlet to triplet excited states in the Pt-containing organic molecules and other heavy metal porphyrins have been observed to be very fast (<200 fs to 1 ps), significantly faster than the lifetime of this feature. We thus assign this Pt–porphyrin GSB signal specifically to the presence of Pt–porphyrin triplet states.^{48–50}

On the basis of the assignments made, we were able to extract the excited state population dynamics from the transient absorption spectra. Specifically, the amplitude of the broad TTP stimulated emission band at 525 nm was used as an assay of TTP singlet excitons. The triplet TTP absorption at 800 nm was determined by subtracting the polymer singlet absorption from the total photoinduced absorption at this wavelength, assuming a negligible triplet yield early (200 fs) after photoexcitation. The triplet photoinduced absorption was

used to estimate the TTP triplet exciton population rise in the films. Finally, the amplitude of the narrow GSB feature of the Pt–porphyrin complex at 510 nm was used as a measure of the triplet state population of this complex. The resulting transient decays are presented in Figure 5.

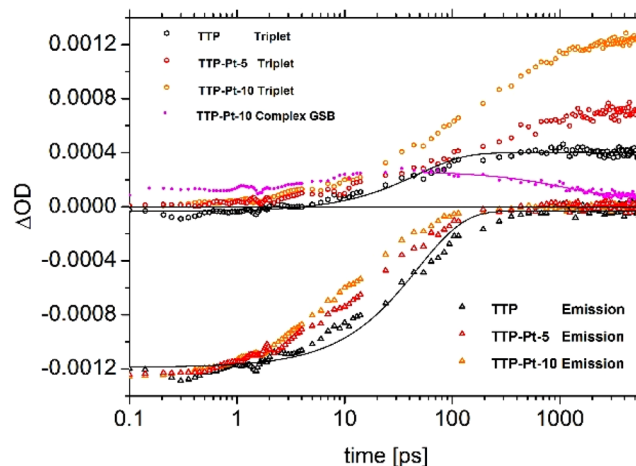


Figure 5. Dynamics of spectral features observed from transient absorption spectra such as that shown in Figure 4, comprising the 525 nm stimulated emission assigned to TTP singlet excitons (triangles), the photoinduced absorption assigned to TTP triplet excitons (circles), and 510 nm GSB signal assigned to Pt–porphyrin triplet states (dotted line). Lines represent least-squares fits of these population dynamics using monoexponential functions.

We focus first on the TTP polymer (Figure 5, black traces). As the stimulated emission of the singlet exciton relaxes (black triangles), the triplet exciton absorption rises (black circles). Both the stimulated emission decay and the TTP triplet rise were fitted with monoexponential functions with a shared time constant of 48.0 ± 1.4 ps, indicating direct population conversion from the singlet to the triplet exciton manifold. This time constant relates to the singlet exciton lifetime in the TTP polymer, in which the triplet excitons are formed via intersystem crossing. Similar lifetimes have previously been reported for other medium bandgap polythiophene polymers such as P3HT.⁵¹ By taking into account the extinction coefficient of the TTP triplet exciton ϵ (800 nm) = $80,000 \text{ M}^{-1} \text{ cm}^{-1}$ (see Supporting Information S4 for calculation of ϵ), we estimated the efficiency of the ISC in the neat polymer to be 20%, calculated from the ratio of the yields of the photoexcited singlet excitons and the generated triplet excitons. Given that

$$\text{ISC}_{\text{efficiency}} = \frac{k_{\text{ISC}}}{k_0}$$

and using our estimates for the singlet exciton decay rate constant k_0 of $(48 \text{ ps})^{-1} = 2.1 \times 10^{10} \text{ s}^{-1}$ and $\text{ISC}_{\text{eff}} = 20\%$, we obtain $k_{\text{ISC}} = (200 \pm 10 \text{ ps})^{-1} = 4.2 \times 10^9 \text{ s}^{-1}$. The relatively high ISC efficiency in the polymer can be attributed to the incorporation of a higher homologue atom (i.e., sulfur, in the polythiophene polymer exhibiting a high spin–orbit coupling constant) or residual palladium from the polymerization.⁵²

The stimulated emission decay in TTP–Pt-10 (Figure 5, orange traces) occurs on a faster time scale compared to neat TTP, as expected from the observed TTP fluorescence quenching in this sample. It is striking that for this film, unlike for the TTP film, the rise of TTP triplet absorption is

significantly delayed relative to the decay of this stimulated emission. The decay of the TTP stimulated emission approximately coincides with the appearance of the Pt–porphyrin GSB, while the rise of the TTP triplet absorption coincides with the decay of this GSB. This is strongly indicative of efficient TTP singlet exciton quenching by the Pt–porphyrin complex on the tens of picoseconds time scale and a subsequent slower back transfer of the complex's triplet state to the polymer (Figure 6).

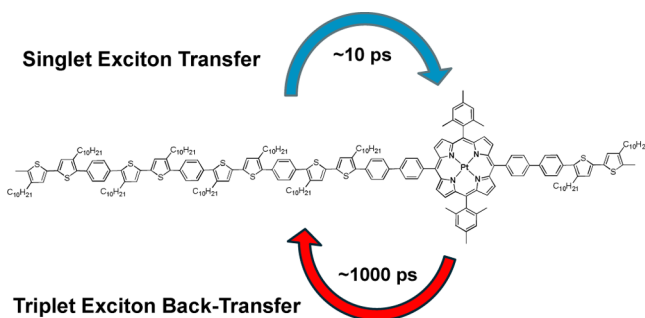


Figure 6. Diagram showing triplet sensitization process.

Pt–porphyrins such as the one studied here are known to undergo very fast and efficient ISC; thus, here we assume that after initial population of the Pt–porphyrin singlet, the porphyrin undergoes extremely fast and efficient ISC, previously estimated to be <200 fs.^{49,50} We also assume a homogeneous distribution of Pt–porphyrin quencher sites in the film because the covalent incorporation of the Pt–porphyrin as a quencher molecule mitigates phase segregation between the materials. Therefore, we used a single exponential function to fit the decay of the Pt–porphyrin GSB, which we associated with the triplet back transfer to the TTP triplet, giving a time constant of 1087 ± 104 ps. Due to spin conservation rules, this triplet energy transfer can only occur via short-range Dexter electron exchange mechanism, which depends strongly on the orbital offset as well as on the orbital overlap between the electron exchanging entities. According to our results, this process is therefore the rate limiting step in the overall process of triplet exciton formation in the TTP–Pt polymers. The time constant for the overall process of TTP triplet formation is of a similar magnitude to the previously reported time constant for mediated triplet exciton formation in polyfluorene–Iridium complex blends: 0.28 ns.⁵³ In addition to the rate constant of triplet population, we also estimated the efficiency of the triplet exciton back transfer by simply taking the ratio of the GSB of the Pt–porphyrin at 5.5 ns and 30 ps, revealing very high polymer triplet exciton generation efficiency of $\sim 60\%$.

One of the properties of triplet excitons in organic semiconductors most relevant to optoelectronic applications is their diffusion length. Here, we carried out transient absorption spectroscopy on the μ s time scale as a function of excitation density to study the decay dynamics of the triplets in the TTP polymer and TTP–Pt-10 (Figure 7). Triplet–triplet exciton annihilation is a well-documented process taking place at increased excitation densities when the encounter of two triplets can lead to the generation of one singlet exciton. This process is strongly dependent on the triplet exciton diffusion constant of the material studied and as such can be used for estimation of triplet exciton diffusion lengths.

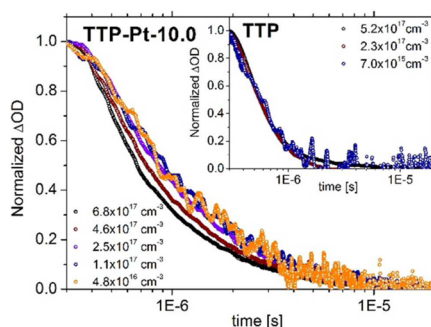


Figure 7. Decay dynamics of the triplet excitons at different initial triplet densities for TTP–Pt-10. The inset shows the corresponding kinetics of the neat TTP polymer. The densities were calculated on the basis of the extinction coefficient of the TTP triplet exciton and the film thickness.

The TTP polymer showed triplet exciton decay completely independent from the initial triplet yield, at least in the range of triplet exciton densities studied here (Figure 7, inset). On the basis of our triplet density dependent decay dynamics, we were able to estimate an upper limit for the triplet exciton diffusion in the TTP. The highest triplet density created upon laser excitation in TTP polymer corresponds to an initial mean separation distance between triplets of 12.4 nm. The absence of any TTA indicates that the triplet exciton diffusion length in the pristine TTP polymer is below this value.

For the TTP–Pt-10 polymer, we observed that the decay dynamics of the triplet excitons is independent of the initial triplet exciton concentration up until an exciton density of $2.5 \times 10^{17} \text{ cm}^{-3}$ is reached. However, upon increasing the initial triplet density to $4.6 \times 10^{17} \text{ cm}^{-3}$ by using higher light excitation density to pump the sample, an accelerated population decay is observed. Notably, the TTA in TTP–Pt-10 occurs at triplet densities which do not cause annihilation processes in the TTP polymer. The triplet excitons in TTP–Pt-10 are formed predominantly due to the energy transfer from the Pt–porphyrin complex and are thus generated in higher densities around the Pt–porphyrin centers. In turn, this inhomogeneous distribution of excitons may result in a higher probability of TTA in TTP–Pt-10 compared to the TTP polymer, where in the latter the triplets are formed via ISC homogeneously. On the basis of these observations, we conclude that the polymer triplet exciton is confined in close proximity to the Pt–porphyrin complex, perhaps due to a low triplet exciton mobility. As noted earlier, we observe the triplet exciton decay for TTP–Pt polymers is biphasic (Figure 3B) and its lifetime is significantly increased ($>3 \mu$ s), whereas the triplet lifetime of the neat TTP polymer is ~ 500 ns only (as determined by monoexponential fitting of its decay (Figure 3B)). The excited state lifetime of Pt–porphyrin complexes is typically $>40 \mu$ s.⁵⁴ This suggests that the triplets generated via the platinum complex are in equilibrium with the triplet state of the complex (Figure 8). The proposition that the Pt–porphyrin and TTP triplet states are in equilibrium is consistent with the observed incomplete triplet back transfer (60%) from the Pt–porphyrin to the TTP backbone. A similar triplet state equilibrium has been reported for conjugated small molecules but has never been demonstrated in a conjugated polymer.^{55,56} Using a Boltzmann distribution, we can therefore estimate the triplet free energy level of the polymer to be ~ 0.06 eV below that of the Pt-complex. The phosphorescence emission maxima

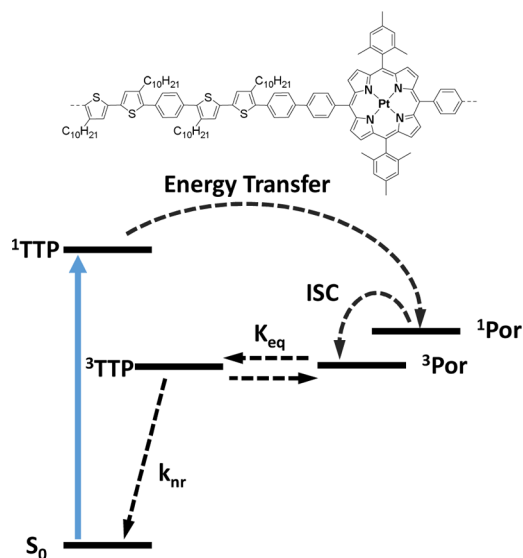


Figure 8. Proposed exciton transfer and equilibration processes in TTP–Pt polymer films.

of Pt–TTP is 1.86 eV and thus, we can estimate the polymer triplet energy level to be ~ 1.93 eV. The S–T gap can subsequently be estimated to be 0.65 eV which is in accordance with studies suggesting that the exchange energy in conjugated polymers is approximately 0.7 eV.^{57,58} Such drastic manipulation of local triplet exciton density and lifetime results in increased T–T annihilation events and has significant implications for triplet–triplet annihilation upconversion layers. It is proposed that utilizing low triplet exciton mobility materials may lead to nondiffusion controlled TTA-UC materials whereby high local triplet density is used to increase upconversion annihilation efficiency.

CONCLUSION

We report the synthesis of a series of novel polythiophene-based semiconducting polymers suitable for efficient polymer triplet exciton generation. The triplet formation is achieved by conversion of the singlet excitons using a host–guest approach, which covalently incorporates heavy metal platinum porphyrin into the conjugated backbone. This approach of incorporating the complex into the polymer backbone allows for an efficient generation of triplet excitons in the polymer material while avoiding potential phase segregation between the polymer backbone and the Pt–porphyrin complex in thin films.

We obtained a detailed photophysical picture of the singlet and triplet exciton dynamics and the triplet exciton formation mechanism using transient absorption spectroscopy. Initial singlet photoexcitations are transferred to the Pt–porphyrin which undergoes ISC. The triplets of the complex are subsequently transferred back onto the polymer triplet energy level with an efficiency of 60% and a time constant of 1087 ± 104 ps, indicating a slow, Dexter electron exchange process as the underlying mechanism. By measuring the triplet density dependent triplet decay dynamics in the TTP polymer, we were able to define an upper limit for the triplet exciton diffusion length of 12.4 nm. We attribute the incomplete triplet backtransfer to an equilibrium between the triplet states of the polymer and the complex which is causing a prolonged polymer triplet exciton lifetime in platinum containing polymers. This results in an increased local triplet exciton

density and increased triplet–triplet annihilation events potentially allowing for a new method of producing upconversion layers.

Our findings show that the sensitization of semiconducting polymers with triplet excitons can be very efficient. This novel materials system allows for determination of almost all the photophysical parameters of a conjugated polymer including estimations for the polymer triplet energy level and triplet diffusion lengths using only spectroscopic methods on thin films. Finally, we demonstrate that this novel host–guest polymeric system can be used to manipulate the spatial distribution of triplet excitons and their lifetime which we believe has significant implications for both triplet sensitized OPV devices and triplet–triplet annihilation upconversion layers.

ASSOCIATED CONTENT

Supporting Information

The Supporting Information is available free of charge on the ACS Publications website at DOI: 10.1021/jacs.5b06223.

Synthetic details and photophysical characterization (PDF)

AUTHOR INFORMATION

Corresponding Authors

*h.bronstein@ucl.ac.uk
*j.durrant@imperial.ac.uk
*m.heeney@imperial.ac.uk

Author Contributions

#These authors contributed equally.

Notes

The authors declare no competing financial interest.

ACKNOWLEDGMENTS

We are grateful to the Imperial College JRF scheme for funding. We are also grateful to the EPSRC, EP/I019278/1, EP/G037515/1 for funding.

REFERENCES

- (1) Köhler, A.; Bäessler, H. *Mater. Sci. Eng., R* **2009**, *66*, 71.
- (2) Adachi, C.; Baldo, M. A.; Thompson, M. E.; Forrest, S. R. *J. Appl. Phys.* **2001**, *90*, 5048.
- (3) Baldo, M. A.; O'Brien, D. F.; Thompson, M. E.; Forrest, S. R. *Phys. Rev. B: Condens. Matter Mater. Phys.* **1999**, *60*, 14422.
- (4) Reineke, S.; Walzer, K.; Leo, K. *Phys. Rev. B* **2007**, *75*, 125328.
- (5) Rao, A.; Chow, P. C. Y.; Gélina, S.; Schlenker, C. W.; Li, C.-Z.; Yip, H.-L.; Jen, A. K. Y.; Ginger, D. S.; Friend, R. H. *Nature* **2013**, *500*, 435.
- (6) Chow, P. C. Y.; Gélina, S.; Rao, A.; Friend, R. H. *J. Am. Chem. Soc.* **2014**, *136*, 3424.
- (7) Westenhoff, S.; Howard, I. A.; Hodgkiss, J. M.; Kirov, K. R.; Bronstein, H. A.; Williams, C. K.; Greenham, N. C.; Friend, R. H. *J. Am. Chem. Soc.* **2008**, *130*, 13653.
- (8) Clarke, T. M.; Durrant, J. R. *Chem. Rev.* **2010**, *110*, 6736.
- (9) Schlenker, C. W.; Chen, K.-S.; Yip, H.-L.; Li, C.-Z.; Bradshaw, L. R.; Ochsenein, S. T.; Ding, F.; Li, X. S.; Gamelin, D. R.; Jen, A. K. Y.; Ginger, D. S. *J. Am. Chem. Soc.* **2012**, *134*, 19661.
- (10) Liedtke, M.; Sperlich, A.; Kraus, H.; Baumann, A.; Deibel, C.; Wirix, M. J. M.; Loos, J.; Cardona, C. M.; Dyakonov, V. *J. Am. Chem. Soc.* **2011**, *133*, 9088.
- (11) Dimitrov, S. D.; Wheeler, S.; Niedzialek, D.; Schroeder, B. C.; Utzat, H.; Frost, J. M.; Yao, J.; Gillett, A.; Tuladhar, P. S.; McCulloch, I.; Nelson, J.; Durrant, J. R. *Nat. Commun.* **2015**, *6*, 6501.

- (12) Soon, Y. W.; Cho, H.; Low, J.; Bronstein, H.; McCulloch, I.; Durrant, J. R. *Chem. Commun.* **2013**, 49, 1291.
- (13) Congreve, D. N.; Lee, J.; Thompson, N. J.; Hontz, E.; Yost, S. R.; Reusswig, P. D.; Bahlke, M. E.; Reineke, S.; Van Voorhis, T.; Baldo, M. A. *Science* **2013**, 340, 334.
- (14) Smith, M. B.; Michl, J. *Annu. Rev. Phys. Chem.* **2013**, 64, 361.
- (15) Rao, A.; Wilson, M. W. B.; Hodgkiss, J. M.; Albert-Seifried, S.; Bässler, H.; Friend, R. H. *J. Am. Chem. Soc.* **2010**, 132, 12698.
- (16) Musser, A. J.; Liebel, M.; Schnedermann, C.; Wende, T.; Kehoe, T. B.; Rao, A.; Kukura, P. *Nat. Phys.* **2015**, 11, 352.
- (17) Zhao, J.; Ji, S.; Guo, H. *RSC Adv.* **2011**, 1, 937.
- (18) Singh-Rachford, T. N.; Castellano, F. N. *Coord. Chem. Rev.* **2010**, 254, 2560.
- (19) Cui, X.; Zhao, J.; Zhou, Y.; Ma, J.; Zhao, Y. *J. Am. Chem. Soc.* **2014**, 136, 9256.
- (20) Reineke, S.; Baldo, M. A. *Sci. Rep.* **2014**, 4, 3797.
- (21) Kohler, A.; Bässler, H. *J. Mater. Chem.* **2011**, 21, 4003.
- (22) Rand, B. P.; Schols, S.; Cheyng, D.; Gommans, H.; Giroto, C.; Genoe, J.; Heremans, P.; Poortmans, J. *Org. Electron.* **2009**, 10, 1015.
- (23) Rand, B. P.; Giroto, C.; Mityashin, A.; Hadipour, A.; Genoe, J.; Heremans, P. *Appl. Phys. Lett.* **2009**, 95, 173304.
- (24) Lee, C.-L.; Hwang, I.-W.; Byeon, C. C.; Kim, B. H.; Greenham, N. C. *Adv. Funct. Mater.* **2010**, 20, 2945.
- (25) Winroth, G.; Podobinski, D.; Cacialli, F. *J. Appl. Phys.* **2011**, 110, 124504.
- (26) Xiong, K.; Hou, L.; Wang, P.; Xia, Y.; Chen, D.; Xiao, B. *J. Lumin.* **2014**, 151, 193.
- (27) Yost, S. R.; Hontz, E.; Yeganeh, S.; Van Voorhis, T. *J. Phys. Chem. C* **2012**, 116, 17369.
- (28) Mikhnenko, O. V.; Blom, P. W. M.; Nguyen, T.-Q. *Energy Environ. Sci.* **2015**, 8, 1867.
- (29) Mikhnenko, O. V.; Ruiter, R.; Blom, P. W. M.; Loi, M. A. *Phys. Rev. Lett.* **2012**, 108, 137401.
- (30) Lebental, M.; Choukri, H.; Chénais, S.; Forget, S.; Siove, A.; Geffroy, B.; Tutiš, E. *Phys. Rev. B* **2009**, 79, 165318.
- (31) Giebink, N. C.; Sun, Y.; Forrest, S. R. *Org. Electron.* **2006**, 7, 375.
- (32) Matsusue, N.; Ikame, S.; Suzuki, Y.; Naito, H. *J. Appl. Phys.* **2005**, 97, 123512.
- (33) Qin, D.; Gu, P.; Dhar, R. S.; Razavipour, S. G.; Ban, D. *Phys. Status Solidi A* **2011**, 208, 1967.
- (34) Tabachnyk, M.; Ehrler, B.; Bayliss, S.; Friend, R. H.; Greenham, N. C. *Appl. Phys. Lett.* **2013**, 103, 153302.
- (35) Irkhin, P.; Biaggio, I. *Phys. Rev. Lett.* **2011**, 107, 017402.
- (36) Samiullah, M.; Moghe, D.; Scherf, U.; Guha, S. *Phys. Rev. B* **2010**, 82, 205211.
- (37) Tamai, Y.; Ohkita, H.; Bente, H.; Ito, S. *Chem. Mater.* **2014**, 26, 2733.
- (38) Luhman, W. A.; Holmes, R. J. *Appl. Phys. Lett.* **2009**, 94, 153304.
- (39) Roberts, S. T.; Schlenker, C. W.; Barlier, V.; McAnally, R. E.; Zhang, Y.; Mastron, J. N.; Thompson, M. E.; Bradforth, S. E. *J. Phys. Chem. Lett.* **2011**, 2, 48.
- (40) Chen, F.-C.; He, G.; Yang, Y. *Appl. Phys. Lett.* **2003**, 82, 1006.
- (41) Chen, F.-C.; Chang, S.-C.; He, G.; Pyo, S.; Yang, Y.; Kurotaki, M.; Kido, J. *J. Polym. Sci., Part B: Polym. Phys.* **2003**, 41, 2681.
- (42) Noh, Y.-Y.; Lee, C.-L.; Kim, J.-J.; Yase, K. *J. Chem. Phys.* **2003**, 118, 2853.
- (43) Jankus, V.; Snedden, E. W.; Bright, D. W.; Whittle, V. L.; Williams, J. A. G.; Monkman, A. *Adv. Funct. Mater.* **2013**, 23, 384.
- (44) Kraft, A.; Grimsdale, A. C.; Holmes, A. B. *Angew. Chem., Int. Ed.* **1998**, 37, 402.
- (45) Fang, L.; Zhou, Y.; Yao, Y.; Diao, Y.; Lee, W.; Appleton, A. L.; Allen, R.; Reinspach, J.; Mannsfeld, S. C. B.; Bao, Z. *Chem. Mater.* **2013**, 25, 4874.
- (46) Ohkita, H.; Cook, S.; Astuti, Y.; Duffy, W.; Tierney, S.; Zhang, W.; Heeney, M.; McCulloch, I.; Nelson, J.; Bradley, D. D. C.; Durrant, J. R. *J. Am. Chem. Soc.* **2008**, 130, 3030.
- (47) Ohkita, H.; Cook, S.; Astuti, Y.; Duffy, W.; Heeney, M.; Tierney, S.; McCulloch, I.; Bradley, D. D. C.; Durrant, J. R. *Chem. Commun.* **2006**, 3939.
- (48) Forster, L. S. *Coord. Chem. Rev.* **2006**, 250, 2023.
- (49) Juban, E. A.; Smeigh, A. L.; Monat, J. E.; McCusker, J. K. *Coord. Chem. Rev.* **2006**, 250, 1783.
- (50) Sheng, C. X.; Singh, S.; Gambetta, A.; Drori, T.; Tong, M.; Tretiak, S.; Vardeny, Z. V. *Sci. Rep.* **2013**, 3, 2653.
- (51) Tamai, Y.; Matsuura, Y.; Ohkita, H.; Bente, H.; Ito, S. *J. Phys. Chem. Lett.* **2014**, 5, 399.
- (52) Janssen, R. A. J.; Smilowitz, L.; Sariciftci, N. S.; Moses, D. J. *Chem. Phys.* **1994**, 101, 1787.
- (53) Liao, H.-H.; Yang, C.-M.; Wu, C.-H.; Horng, S.-F.; Lee, W.-S.; Meng, H.-F.; Shy, J.-T.; Hsu, C.-S. *Appl. Phys. Lett.* **2007**, 90, 013504.
- (54) Moiseev, A. G.; Margulies, E. A.; Schneider, J. A.; Belanger-Gariepy, F.; Perepichka, D. F. *Dalton Trans.* **2014**, 43, 2676.
- (55) Whited, M. T.; Djurovich, P. I.; Roberts, S. T.; Durrell, A. C.; Schlenker, C. W.; Bradforth, S. E.; Thompson, M. E. *J. Am. Chem. Soc.* **2011**, 133, 88.
- (56) Baldo, M. A.; Forrest, S. R. *Phys. Rev. B: Condens. Matter Mater. Phys.* **2000**, 62, 10958.
- (57) Monkman, A. P.; Burrows, H. D.; Hartwell, L. J.; Horsburgh, L. E.; Hamblett, I.; Navaratnam, S. *Phys. Rev. Lett.* **2001**, 86, 1358.
- (58) Köhler, A.; Beljonne, D. *Adv. Funct. Mater.* **2004**, 14, 11.